

## MODELING BORON ADSORPTION ON KAOLINITE

SHIVI P. N. SINGH<sup>1</sup> AND SHAS V. MATTIGOD<sup>2</sup>

<sup>1</sup> United Engineers and Constructors, Denver, Colorado 80217

<sup>2</sup> Battelle, Pacific Northwest Laboratories, Richland, Washington 99352

**Abstract**—Boron adsorption at constant ionic strength [ $0.09 \pm 0.01$  moles/liter of  $\text{KClO}_4$  or  $\text{Ca}(\text{ClO}_4)_2$ ] on 0.2–2  $\mu\text{m}$  clay fraction of pretreated kaolinite was modeled using both phenomenological equations and surface complexation reactions. Phenomenological equations were expressed as linear relationships between the distribution coefficient and adsorption density or equilibrium concentration. The normalized form of the isotherms allowed the distribution coefficient to be predicted over a wide range of adsorption densities or equilibrium concentrations and pH. The Langmuir isotherm revealed a weak two-part linear trend supported by a similar behavior of the van Bemmelen-Freundlich isotherm. Potential adsorption mechanisms were assessed from these isotherms. The bases for the inner-sphere (surface coordination) and outer-sphere (ion-pair) surface reactions were postulated, and equations were developed and incorporated into the generalized triple-layer surface-complexation model [TL(g)-SCM]. Boron adsorption was best modeled using the inner-sphere complexes. The results confirm that the generalized triple-layer surface-complexation model can provide information regarding plausible reactions at the substrate/aqueous interface. Intrinsic constants for postulated surface reactions were derived as fitting parameters over a range of pH and initial boron concentrations.

**Key Words**—Adsorption, Boron, Ion-pair, Ion-speciation, Kaolinite, Surface complexation, Triple-layer model.

### INTRODUCTION

Equilibrium adsorption studies conducted in laboratory model systems have provided the basis for the understanding of the surface chemistry of minerals. The bulk of the thermodynamic data extracted from these equilibrium adsorption studies has been based on experimental observations of metal-ion adsorption onto well-characterized substrates, consisting predominantly of metal-oxides. Models using highly detailed laboratory information have been widely applied for the oxide-solution interfacial reactions. Extensive studies of boron adsorption and fixation on clay minerals have stemmed from boron's importance as an essential micronutrient, paleosalinity indicator, and trace component of fossil fuel wastes. There is, however, limited evidence of the application of these models to boron adsorption on kaolinite. This paper will attempt to address the application of these detailed modeling techniques to boron adsorption on kaolinite using the published experimental data of Mattigod *et al.* (1985).

The application of the concepts and mathematical formalism of coordination chemistry to ion-particle interaction forms the basis of the surface-coordination or site-binding models. These models incorporate explicit solution speciation and reaction stoichiometry, and are therefore useful devices for understanding the physico-chemical nature of the surface-complexation reactions. The constant capacitance surface complexation model (CC-SCM) has been used by Goldberg and Glaubig (1985, 1986) to predict boron adsorption behavior on oxides and clay minerals including kaolinite.

Mattigod *et al.* (1985) studied the effect of ion-pair formation on boron adsorption by kaolinite, but made no attempt to model the phenomenon.

The adsorption and fixation of ions onto kaolinite is not fully understood. The hydroxylated edge and defect sites of kaolinite provide potential sites for ion adsorption. Because of the complex surface chemistry, few investigators have linked the quantitatively measured surface properties of kaolinite with boron adsorption. Past studies were qualitative, since the observed effects of individual experimental and measured surface parameters, as well as the nature of the surface on the adsorption process were presented without quantifying the variables (Bassett, 1976). Recent studies include the development and application of a phenomenological equation (Keren and Mezuman, 1981) and the CC-SCM (Goldberg and Glaubig, 1985, 1986) to simulate boron adsorption. The triple-layer surface complexation model (TL-SCM) has been applied by Zachara *et al.* (1987, 1988) to model chromate adsorption on amorphous iron oxyhydroxide and kaolinite. Hayes and Leckie (1987) and Hayes *et al.* (1988) studied the ionic strength effects of both cation and anion adsorption on iron oxide, using the generalized triple-layer surface complexation model (TL(g)-SCM). Previous use of TL-SCM and TL(g)-SCM for adsorption of anions onto various substrates suggests the applicability of these models to boron adsorption on kaolinite.

In this paper, the published data for boron adsorption on kaolinite by Mattigod *et al.* (1985) have been used to evaluate the application of TL(g)-SCM and to

provide an understanding of boron adsorption on kaolinite. Phenomenological descriptions have also been evaluated to provide an understanding of heterogeneous sites for adsorption. Parameters, such as surface area, surface site density, and surface reaction constants applicable for the SCM were retrieved from published data.

### BORON ADSORPTION

The interaction of kaolinite with weak acids in aqueous solution is highly dependent on pH, since the charge generation reaction at the interface and the dissociative reaction of the weak acid is influenced by the pH. The affinity of kaolinite for the adsorbing species decreases beyond the maximum adsorption values located close to the  $pK_a$  of the acid. These adsorption profiles have been interpreted qualitatively on the basis of the expected changes in the chemical, electrostatic, and solvation effects of the Gibbs adsorption energy. Interfacial reactions involving the displacement of the surface hydroxyl groups by the adsorbing anion (Sposito, 1984) can be written as:



where  $S-OH$  represents the surface hydroxyls,  $LH_q^{-n}$  the adsorbing ligand, and  $S-LH_q^{-(n-1)}$  the adsorbed surface-ligand complex.

The surface charge density is not totally accounted for by the above reaction, which must be supplemented with other intermediate reactions depending on the protolytic equilibria of  $LH_q^{-n}$  obtained from potentiometric titration experiments. Boron adsorption data on soils, in general, have been interpreted in terms of differing affinity of the surface group for the uncharged boron species  $B(OH)_3^0$  below pH 7 and its predominant anionic species  $B(OH)_4^-$  above pH 7 (Baes and Mesmer, 1976), giving rise to an adsorption maximum around pH 9. Based on experimental evidence and comparison with the results of other investigators, Mattigod *et al.* (1985) proposed that enhanced boron adsorption in the presence of  $Ca^{2+}$  over that in solutions dominated by monovalent cations is due to the adsorption of the  $CaB(OH)_4^+$  ion-pair.

Goldberg and Glaubig (1985, 1986) used the CC-SCM (Stumm *et al.*, 1970, 1976, 1980; Sigg and Stumm, 1981; Schindler and Gamsjäger, 1972) to model specific adsorption of boron onto kaolinite and other clay minerals. The CC-SCM treats specific adsorption as ligand exchange through inner-sphere complexation. The "intrinsic" conditional equilibrium constants are extrapolated conditional equilibrium values at zero net surface charge referenced to a constant ionic strength medium. These constants are valid only for the specific set of experimental conditions. Therefore, the CC-SCM application is limited to simpler models, systems, and specific experimental data. In the application of the CC-SCM, Goldberg and Glaubig (1985, 1986) assumed

that the reactive functional groups protonate and dissociate, thus allowing boron to adsorb through a ligand exchange mechanism only with the reactive surface aluminol groups located at the edge of the kaolinite platelets. Species such as  $AlH_3BO_3^+$  (S) and  $AlHBO_3^-$  (S), were considered in their optimization studies but were shown to be of minor importance. These species were omitted from the model, reducing the model to a single reaction for boron adsorption on kaolinite. The plateau predicted by CC-SCM in the pH range of 6.8–9.0 does not agree with the observed boron adsorption maximum in the pH range of 8.0–9.0 (Goldberg and Glaubig, 1985, 1986). The inherent limitations of the CC-SCM model to include outer-sphere complexation for electrolyte adsorption effects and the use of a single reaction may have resulted in this type of predicted adsorption curve.

Keren and Mezuman (1981) developed an equation that incorporated the effect of pH and solution-boron speciation to fit the experimental data. The intrinsic constants extracted were defined as an affinity parameter for the interactions of boron valid for a constant ionic strength. The authors proposed that boron adsorption occurred through a ligand exchange mechanism with the surface hydroxyl groups.

Boric acid is not a Lewis acid but it reacts with the hydroxyl ions to form an oxyanion, which has been shown to adsorb specifically to substrates. Experimental observation of a shift of the zero potential charge (ZPC) following boron adsorption has been observed on boehmite (Fricke and Leonhardt, 1950), pseudo-boehmite (Alwitt, 1972), aluminum hydroxide gel (Beyrouy *et al.*, 1984) and magnetite (Blesa *et al.*, 1984) indicating specific adsorption on these minerals. It is within this context that boron adsorption on kaolinite has been investigated and surface reactions formulated to interpret the surface interactions from experimental observations. The capability of TL(g)-SCM to describe the adsorption behavior was evaluated, and the phenomenological formulations were also applied to provide supporting information.

### MATERIALS AND METHODS

A brief description of the results of the detailed experiment conducted by Mattigod *et al.* (1985) is provided here. Well-crystallized Washington County, Georgia kaolinite (KGa-1) was pretreated to remove any surface oxide and hydroxide coatings (Sposito *et al.*, 1981). Chemical analysis of this clay fraction (0.2–2  $\mu m$ ) indicated a clay composition of 44.2%  $SiO_2$  and 39.7%  $Al_2O_3$  versus an ideal kaolinite composition of 46.5%  $SiO_2$  and 39.5%  $Al_2O_3$ , respectively. Boron incorporated within the kaolinite was determined to be 132  $\mu g/g$  of which less than 1  $\mu g/g$  was extractable by 0.01 M mannitol, 0.033 M  $Ca(ClO_4)_2$  or 0.2 M ammonium-oxalate.

Boron adsorption studies were conducted using a



0.2–2.0  $\mu\text{m}$  fraction of kaolinite at a temperature of  $25^\circ \pm 2^\circ\text{C}$  over the pH range of 6 to 10.5. The electrolyte ionic strength of either  $\text{KClO}_4$  or  $\text{Ca}(\text{ClO}_4)_2$  were kept constant at  $0.09 \pm 0.01$  moles/liter during the experiment. Equilibration time of boron adsorption in polycarbonate centrifuge tubes under a nitrogen atmosphere was established as 20 hours at  $25^\circ\text{C}$ . Average concentration of 0.71 mg/liter of Al and 0.39 mg/liter of Si at pH 10.5 was observed in the supernatant.

#### PHENOMENOLOGICAL DESCRIPTION OF ADSORPTION

The success of surface-complexation models (SCMs) as heuristic devices in aqueous chemistry for explaining solute-particle interactions has been limited by the detailed information required for their implementation. These surface-complexation models have often been supplanted in practice by the phenomenological equations that retain their generic relationship among master variables inherent in the SCMs. Phenomenological models are based on net changes in the system composition and unlike surface-complexation models do not quantify the details of the surface interactions explicitly. Included within this group are distribution coefficients, isotherms, and apparent adsorbate/proton exchange stoichiometries. These models, although limited in their information, often provide evidence for the existence of heterogeneous adsorption sites.

A simple association reaction can be defined for the distribution coefficient,  $K_d$ , as:

$$K_d = \frac{[C_{\text{ads}}]}{[C_{\text{aq}}][C_p]} \text{ (ml/g)}, \quad (2)$$

where  $[\ ]$  denotes concentration,  $C_p$  the particle concentration,  $C_{\text{aq}}$  the equilibrium concentration of all the species of interest in the solution, and  $C_{\text{ads}}$  the quantity adsorbed on the particle surface.  $C_e$  (see below) is used synonymously with  $C_{\text{aq}}$ . The value of  $K_d$  is generally limited to the experimental results and a specific pH.

The Langmuir isotherm can be derived in a variety of forms. Implicitly embedded in the derivation are the assumptions that surface sites are homogeneous and the surface interaction energy is not altered by the adsorption density. According to Sposito (1984), the Langmuir relationship can be expressed in terms of the distribution coefficient and adsorption density:

$$K_d = k_L S_T - k_L \Gamma, \quad (3)$$

where  $k_L$  is the Langmuir intrinsic binding (association) constant,  $S_T$  the total surface sites and  $\Gamma$  the adsorption density. Thus, a  $K_d$ -versus-adsorption density plot is linear when the adsorbed concentration on the surface is well below  $S_T$ . The normalized form of Eq. (3) can be expressed as:

$$K_d = k_L S_T - (k_L C_i) \left( \frac{\Gamma}{C_i} \right), \quad (4)$$

where  $C_i$  is the initial concentration. The Langmuir constants were determined by plotting  $K_d$  vs  $(\Gamma/C_i)$ .

The van Bemmelen-Freundlich isotherm, which accounts for surface-site heterogeneity and surface interaction energy, in terms of similar variables used in Eqs. (3) and (4) is:

$$K_d = k_F [C_e]^{(1/n-1)}, \quad (5)$$

where  $C_e$  is the equilibrium concentration,  $k_F$  and  $1/n$  are adjustable parameters (Sposito, 1984). Normalizing Eq. (5) yields:

$$K_d = k_F [C_i]^{(1/n-1)} \left( \frac{C_e}{C_i} \right)^{(1/n-1)}. \quad (6)$$

By plotting  $K_d$  as a function of  $C_e/C_i$ , the van Bemmelen-Freundlich constants were determined. The above isotherms in the form of Eqs. (4) and (6) were used in this study to analyze the adsorption behavior of boron over the entire range of pH and initial concentration.

#### SURFACE-COMPLEXATION MODELS

Surface complexation models, developed on the concepts and mathematical formalism of coordination chemistry, have been successfully used to simulate adsorption interaction at the solid/aqueous interface. The TL-SCM (Davis and Leckie, 1979, 1980) have been widely applied to adsorption isotherms of cations and anions. The TL(g)-SCM, which incorporates the modeling features of both the TL-SCM and CC-SCM, can simultaneously predict adsorption behavior of aqueous sorbate species and the development of the surface charge at hydrous oxide interfaces using a single set of equilibrium constants. The TL-SCM and TL(g)-SCM are comprehensive models applied with reasonable success to predict cation and anion adsorption in dilute to moderately concentrated solutions (Davis and Leckie, 1978, 1979, 1980; Balistrieri and Murray, 1979; Zachara *et al.*, 1987, 1988). These models have also been used to predict the ionic strength effects on cation ( $\text{Pb}^{2+}$ ,  $\text{Cd}^{2+}$ ) and anion ( $\text{SeO}_3^{2-}$ ,  $\text{SeO}_4^{2-}$ ) sorption on ferrous oxides (Hayes and Leckie, 1987; Hayes *et al.*, 1988).

The Gouy-Chapman description of the electrical double layer (EDL) as modified by Stern-Grahame (1947) forms the basis for the TL(g)-SCM used in this paper and differs from the original surface complexation models in two basic aspects. First, the adsorbed ions were considered as ion-pair complexes at the  $\beta$ -plane within the EDL based on the original formulation and interpretation of the TL-SCM. In this paper, adsorbed ions, which are considered inner- and outer-sphere complex analogs, can form surface complexes at either the O- or the  $\beta$ -plane (Figures 1, 2). Second, the chemical potential, as well as the standard and reference states, are defined equivalently for both the

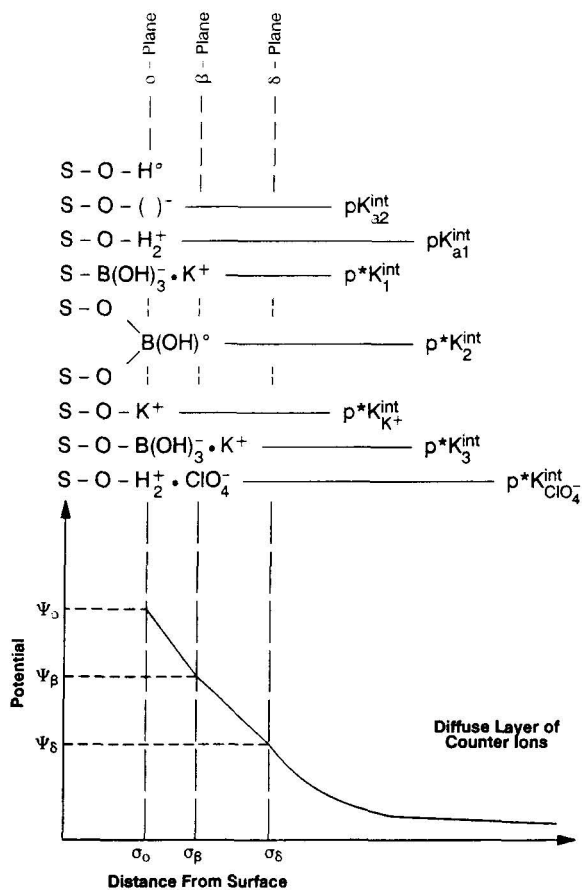


Figure 1. Representation of the kaolinite/aqueous electrolyte (KClO<sub>4</sub>) interface for boron adsorption within the TL(g)-SCM.

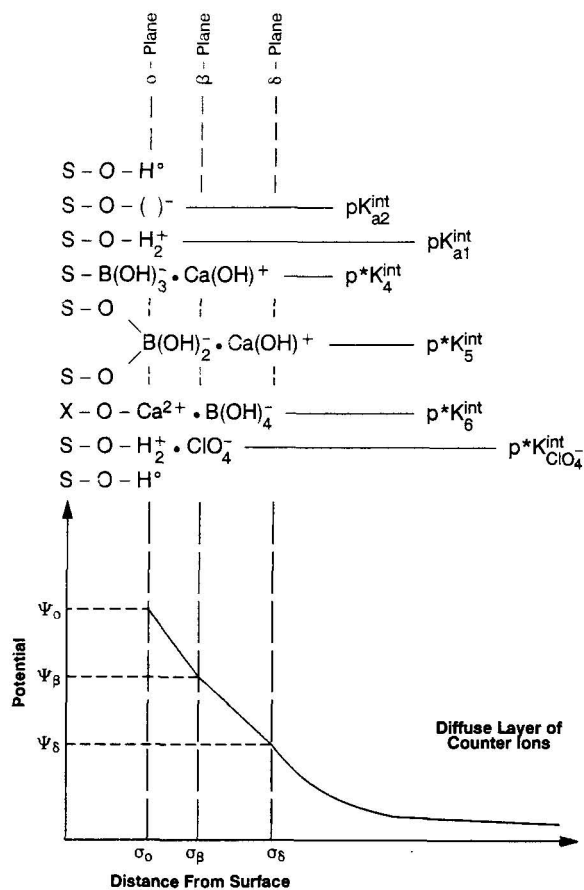


Figure 2. Representation of the kaolinite/aqueous electrolyte [Ca(ClO<sub>4</sub>)<sub>2</sub>] interface for boron adsorption within the TL(g)-SCM.

solution and surface species, leading to a different relationship between the activity coefficients and the interfacial potential than the original development. The TL(g)-SCM has been successfully used by Hachiya *et al.* (1984) for modeling adsorption of divalent cations on γ-Al<sub>2</sub>O<sub>3</sub> at constant ionic strength, while Richter (1987), Swallow *et al.* (1980), and Hayes and Leckie (1987) studied the effects of strongly sorbed ions.

The detailed thermodynamic basis of surface complexation (Hayes and Leckie, 1986) is illustrated using the surface protolysis reaction:



Application of the standard chemical potential to each component X [= SOH<sub>2</sub><sup>+</sup>, SOH, TOH<sub>2</sub><sup>+</sup>, TOH or H<sup>+</sup>], is given by:

$$\mu_x = \mu_x^0 + RT \ln[X] + \ln[\gamma_x] \quad (8)$$

For each species X, μ and μ<sup>0</sup> are the chemical and the standard state chemical potential, respectively. [X] is the concentration and γ<sub>x</sub> is the activity coefficient defined such the γ = 1 at the reference state condition.

R and T are the ideal gas constant and temperature, respectively. The macroscopic thermodynamic constant formulation of the reaction stated in Eq. (7) is:

$$K_{ax}^0 = \frac{[\text{SOH}][\text{H}^+]\gamma_{\text{SOH}}\gamma_{\text{H}^+}}{[\text{SOH}_2^+]\gamma_{\text{SOH}_2^+}} \quad (9)$$

Additionally, solvent electrical properties over significant distances are affected by surface charge. Thus separation of activity correction (Davis and Leckie, 1978) into "chemical" and "coulombic" contributions can be incorporated for the surface species to define the electrochemical potential. Using Eq. (8) for surface species leads to:

$$\bar{\mu}_{xs} = \bar{\mu}_{xs}^0 + RT(\ln[X_s] + \ln[\gamma_{xs}]) + Z_{xs}F\phi \quad (10)$$

For the surface species X, μ̄ and μ̄<sup>0</sup> are the electrochemical potential and the electrochemical potential at the standard state, respectively. X<sub>s</sub> is the surface concentration, γ<sub>xs</sub> is the surface activity coefficient due to "chemical" effects, Z<sub>xs</sub> is the charge of the surface species, F is the Faraday constant, and φ is the elec-



trostatic potential. The term  $Z_{xs}F\phi$  is the "coulombic" activity due to the difference in surface and solution potential. Using Eq. (10), the intrinsic acidity constant is defined as:

$$K_{ax}^* = \frac{[\text{SOH}][\text{H}^+]\gamma_{\text{SOH}}\gamma_{\text{H}^+}\exp(-ZF\psi_0/RT)}{[\text{SOH}_2^+]\gamma_{\text{SOH}_2^+}} \quad (11)$$

$\psi_0$  is the average potential of the surface plane. The  $\gamma_x$  and  $\gamma_{xs}$  are defined similarly (Chan *et al.*, 1975; Sposito, 1984). In various SCMs, and the TLM as applied by Davis *et al.* (1978), the surface activity is related to the surface activity at zero ionic strength by an exponential term that incorporates the average potential of the plane:

$$\gamma_{xs} = \gamma_{0xs} \exp(ZF\psi_0/RT) \quad (12)$$

A modified development for the TL(g)-SCM is used in this paper. The same standard for reference states are chosen for both the surface and solution species, consistent with the concept that surface-complexation models treat surface functional groups as constrained ligands in solution. The standard state is selected as 1 mole/liter and the reference state is infinite dilution relative to the aqueous phase at zero surface charge. Zero surface charge eliminates ion interactions of either solution of surface species. This permits thermodynamic constants to be obtained by extrapolation of the titration data to zero surface charge. The surface and solution activity coefficients are not separated in the modeling concept used in this paper. Instead, a common potential is defined for both solution and surface species X:

$$\mu_x = \mu_x^0 + RT \ln[X] + Z_x F \phi_x, \quad (13)$$

where  $\mu_x$  and  $\mu_x^0$  are the chemical potentials defined in Eq. (8). The  $Z_x F \phi_x$  term, however, represents the free energy required to bring a charge,  $Z$ , from the reference state potential to the given potential.  $F$  is the Faraday constant and  $\phi$  the potential. Several thermodynamic developments that signify important differences from the previous descriptions are delineated. The thermodynamic constant equation is formulated by applying Eq. (13) to each species X in Eq. (7) to obtain the chemical potential for the individual species. The summation of the chemical potential for the species is given by:

$$\Delta\mu_x = \Delta\mu_x^0 + RT \ln([\text{SOH}][\text{H}^+]/[\text{SOH}_2^+]) + \sum Z_x F \phi_x. \quad (14)$$

Defining the following relationships:

$$\Delta\mu = \Delta\mu_{\text{SOH}} + \Delta\mu_{\text{H}^+} - \Delta\mu_{\text{SOH}_2^+} \quad (15)$$

$$\Delta\mu^0 = \Delta\mu_{\text{SOH}}^0 + \Delta\mu_{\text{H}^+}^0 - \Delta\mu_{\text{SOH}_2^+}^0, \quad (16)$$

and applying the equilibrium condition,  $\Delta\mu = 0$ , the difference in the chemical potentials lead to the formulation of the TL(g) intrinsic equilibrium constant:

$$K_{ax}^0 = \frac{[\text{SOH}][\text{H}^+]}{[\text{SOH}_2^+]} \exp[F(\phi_{\text{H}^+} - \phi_{\text{SOH}_2^+})/RT]. \quad (17)$$

The TL(g)-SCM potential  $\psi_0$  is the potential difference of the surface and the bulk species that alters the thermodynamic constant to:

$$K_{ax}^0 = \frac{[\text{SOH}][\text{H}^+]}{[\text{SOH}_2^+]} \exp(-F\psi_0/RT). \quad (18)$$

A relation between the activities and the exponential term containing the potential can be formulated by comparing the above equation with Eq. (9):

$$\frac{\gamma_{\text{SOH}}\gamma_{\text{H}^+}}{\gamma_{\text{SOH}_2^+}} = \exp(-F\psi_0/RT). \quad (19)$$

From Eq. (13), it can be shown that  $\gamma_{\text{SOH}} = 1$  when the surface charge  $Z_{\text{SOH}} = 0$ . The ratio of the activity coefficient of the surface and the bulk species are related by the exponential term. In Eq. (12) the relationship is limited to the surface activity coefficients at the experimental and zero ionic strength. Thus the relationship in the present development (Eq. 20) links the ratio of the activity coefficients to the potential and charge differential of the solution and the adsorbed species:

$$\frac{\gamma_{\text{H}^+}}{\gamma_{\text{SOH}_2^+}} = \exp(-F\psi_0/RT). \quad (20)$$

The surface charge, in the TLM, is also related to the surface potential,  $\psi_0$ , and  $\beta$ -layer potential,  $\psi_\beta$ , by the interlayer capacitance:

$$\sigma_0 = C_l [\psi_0 - \psi_\beta]. \quad (21)$$

The surface acidity and the electrolyte intrinsic constants are determined by extrapolation of the potentiometric titration data to zero surface charge. At zero surface charge and low ionic strength [ $\psi_\beta \approx 0$ ], the surface potential is zero. Hence, the extrapolated acidity constants and thermodynamic constants are equal. Similarly, for the electrolyte binding constants at zero surface charge, the potential difference [ $\psi_0 - \psi_\beta$ ] is zero and the exponential term is reduced to one, establishing the equivalence of the intrinsic and the thermodynamic constants based on the reference and standard states defined for the TL(g)-SCM. The above thermodynamic basis applied to the surface protolysis reaction of Eq. (7) forms the basis of the mass action and activity coefficient relationship of the other reactions. Similar thermodynamic development for other surface reactions were used to formulate the mass and activity coefficient relationship.

## MODELING PARAMETERS

The constant ionic strength adsorption isotherm data for the electrolytes  $\text{KClO}_4$  and  $\text{Ca}(\text{ClO}_4)_2$  as a function of concentration were obtained from Mattigod *et al.*

Table 1. Stability constants of soluble complexes at 25°C.

Reactions	Log (K)	Reference
$H^+ + B(OH)_4^- = B(OH)_3^0 + H_2O$	9.24	Mesmer <i>et al.</i> (1972)
$K^+ + B(OH)_4^- = KB(OH)_4^0$	0.00	Bryne and Kester (1974)
$Ca^{2+} + B(OH)_4^- = CaB(OH)_4^+$	9.24	Reardon (1976)
$Ca^{2+} + OH^- = CaOH^+$	-12.60	Mesmer <i>et al.</i> (1972)
$K^+ + OH^- = KOH^0$	-11.60	Mesmer <i>et al.</i> (1972)

(1985). Other input parameters required for modeling the TL(g)-SCM were taken from Davis and Leckie (1978, 1980), Riese (1982), Mattigod *et al.* (1985) and Zachara *et al.* (1988). FITEQL (Westall, 1982), a computer program developed for the application of adsorption at charged interfaces with surface-complexation models, was used to model surface reactions and compute the intrinsic equilibrium constants from the experimental boron adsorption envelope. The activity coefficients for adjusting the input parameters were calculated by the Davies equation (1962). The kaolinite structure was assumed as ideal, without isomorphous substitution. Aluminol and silanol edge sites were assumed proportional to the clay composition determined by chemical analysis (Mattigod *et al.*, 1985) to account for the total site density. Due to insignificant clay dissolution (0.71 Al, 0.39 Si mg/liter), speciation computations were not affected. However, differences in treatment and probable dissolution not accounted for may affect the acidity and the conditional equilibrium constants taken from Riese (1982). The surface parameters, acidity constants, and conditional equilibrium constants from the available literature have been used at this stage without attempting to verify the validity of these numbers. The stability constants of soluble complexes, surface parameters, and the surface reaction parameters needed for modeling the system are tabulated (Tables 1–3). The surface complexation constants are summarized in Table 4. The equations form a self-consistent set of subreactions for use in surface-complexation models, for a system containing the components SOH, OH<sup>-</sup>, B(OH)<sub>3</sub><sup>0</sup>, B(OH)<sub>4</sub><sup>-</sup>, K<sup>+</sup>, Ca<sup>2+</sup> and ClO<sub>4</sub><sup>-</sup>. The notation O and β represent triple-layer-model planes (Figures 1, 2) within the EDL, which are specifically identified in the model structure. The ψs represent the potential at those planes.

## RESULTS AND DISCUSSION

### Phenomenological equations

It is well established in simple systems that the principal factors controlling the adsorption density in the experiments are the equilibrium solution concentration and pH. The equilibrium solution concentration is dependent on the amount adsorbed, the ion-pair effect, and the initial concentration. To reduce the isotherms to a single curve irrespective of the differences exhibited, the ratio of the individual variables (adsorption density, equilibrium concentration) to the initial concentration was used in the construction of the plots (Figures 4, 5). Regression analyses of the data in these plots are presented in Table 5. All the isotherms exhibit a linear trend. The minimum and maximum distribution coefficient or adsorption density for boron adsorption in Ca(ClO<sub>4</sub>)<sub>2</sub> electrolyte exceeds those in KClO<sub>4</sub> medium.

The surface species cannot be explicitly modeled in the isotherms. Since the adsorbed species are often treated as analogs of the species in the solution, incorporation of solution species as a function of pH into K<sub>d</sub> provides an insight into the selective adsorption effect. An apparent distribution K<sub>dA</sub> in terms of K<sub>d</sub> can be derived as:

$$K_{dA} = [K_d][K_{pHS}]^{-1}.$$

K<sub>pHS</sub>, under simplifying assumptions, can be formulated to incorporate the effect of solution speciation as a function of pH. It is expressed as:

$$K_{pHS} = [1 + 10^{pH+pK_{aB}}(1 + \gamma_s K_s [C_s])]$$

where s is the cation, K<sup>+</sup> or Ca<sup>2+</sup>. The difference of (K<sub>pHS</sub>)<sup>-1</sup> of these two cations is illustrated in Figure 3 and shows a peak around pH 9. This indicates the effect

Table 2. Parameters for the surface-complexation model.

Parameter	Value	Reference
Surface area (m <sup>2</sup> /g)	25.00 ± 3	Mattigod <i>et al.</i> (1985)
Solids (g/liter)	51–56	Mattigod <i>et al.</i> (1985)
Surface site density (sites/nm <sup>2</sup> )	6.00	Riese (1982)
Capacitances (F/cm <sup>2</sup> ):		
Inner layer (C1)	120–240	Zachara <i>et al.</i> (1987)
Outer layer (C2)	20	Davis and Leckie (1978)



Table 3. Surface reaction constants.

Reaction	Log ( $K_{int}$ )	Reference
$SiOH + H^+ = SiOH_2^+$	-1.75	Riese (1982)
$SiOH = SiO^- + H^+$	-6.25	Riese (1982)
$SiOH + K^+ = (SiO^- \cdot K^+)^0$	-1.75	Riese (1982)
$SiOH + Ca^{2+} = (SiO^- \cdot Ca^{2+})^+$	-1.75	Riese (1982)
$AlOH + H^+ = AlOH_2^+$	-5.70	Davis and Leckie (1978)
$AlOH = AlO^- + H^+$	-11.4	Davis and Leckie (1978)
$AlOH + K^+ = (AlO^- \cdot K^+)^0$	-9.15	Riese (1982)
$AlOH + Ca^{2+} = (AlO^- \cdot Ca^{2+})^+$	7.40	Riese (1982)
$AlOH + H^+ + ClO_4^- = (AlOH_2^+ \cdot ClO_4^-)^0$	-1.75	Davis and Leckie (1982)

of the cation species  $[Ca^{2+}B(OH)_4]^-$  on boron adsorption onto kaolinite. This inference, however, does not distinguish between adsorption effects of the ion-pair and exchangeable cation.

#### Langmuir isotherm

The Langmuir isotherm (Figure 4) is linear at low adsorption density but exhibits a weakly non-linear behavior with increasing pH and minimum equilibrium concentration around pH of 8.5–9 for  $KClO_4$  and 9.0 for  $Ca(ClO_4)_2$ , close to the pKa (9.24) of the boric acid. The non-linear trend again is more strongly exhibited in the  $Ca(ClO_4)_2$  electrolyte. Two regression

analyses were conducted. The total data set was used in the first analysis. In the second analysis, the distribution coefficients at high adsorption densities were eliminated from the analysis. The data sets not considered in the analysis were predominantly from the experimental results of boron adsorption in the  $Ca(ClO_4)_2$  electrolyte. The second regression analysis showed an improved correlation confirming the non-linearity observed at high adsorption density. The adsorption of the divalent calcium onto silanol sites creates positive sites for the adsorption of the oxyanion of boron. The ion-pair effect also enhances the potential for adsorption onto negatively-charged sites, thus creating a nonlinear trend at high adsorption densities.

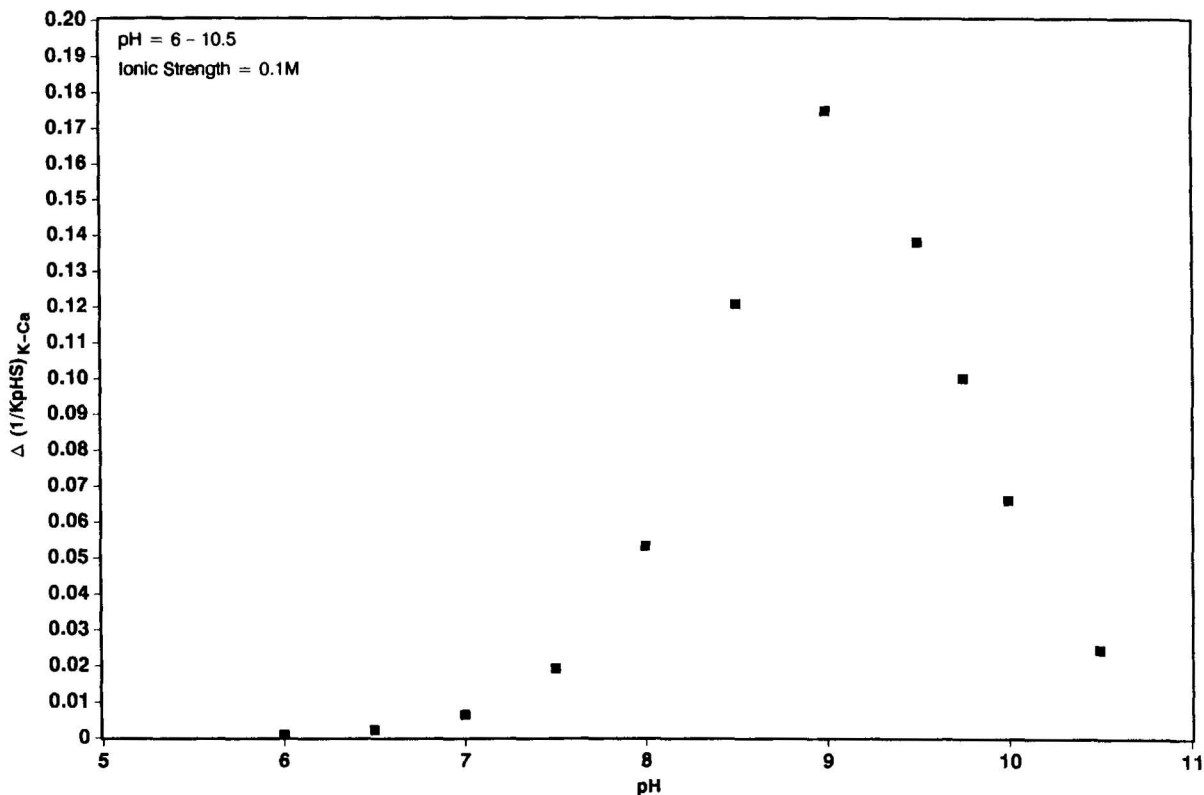


Figure 3. Speciation pH effect of boron on distribution coefficient.

Table 4. Equations for surface-complexation reactions.

Surface protolysis reactions	Equilibrium equations
$\text{SOH}_2^+ = \text{SOH} + \text{H}^+$	$K_{a1}^* = \frac{[\text{SOH}][\text{H}^+]}{[\text{SOH}_2^+]} \exp[-F^*(\psi_0)]$
$\text{SOH} = \text{SO}^- + [\text{H}^+]$	$K_{a2}^* = \frac{[\text{SO}^-][\text{H}^+]}{[\text{SOH}]} \exp[-F^*(\psi_0)]$
<b>Electrolyte surface complexation reactions</b>	
$\text{SOH} + \text{K}^+ = [\text{SO}^- - \text{K}^+] + [\text{H}^+]$	$K_{\text{K}}^* = \frac{[\text{SO}^- - \text{K}^+][\text{H}^+]}{[\text{SOH}][\text{K}^+]} \exp[F^*(\psi_\beta - \psi_0)]$
$\text{SOH} + \text{Ca}^{2+} = [\text{SO}^- \text{Ca}^{2+}]^+ + [\text{H}^+]$	$K_{\text{Ca}}^* = \frac{[\text{SO}^- \text{Ca}^{2+}][\text{H}^+]}{[\text{SOH}][\text{Ca}^{2+}]} \exp[F^*(\psi_0)]$
$\text{SOH} + \text{H}^+ + \text{ClO}_4^- = \text{SOH}_2^+ - \text{ClO}_4^-$	$K_{\text{ClO}_4}^* = \frac{[\text{SOH}_2^+ - \text{ClO}_4^-]}{[\text{SOH}][\text{H}^+][\text{ClO}_4^-]} \exp[F^*(\psi_0 - \psi_\beta)]$
<b>Boron surface complexation reactions</b>	
$\text{SOH} + \text{B}(\text{OH})_3^0 + \text{H}^+ + \text{K}^+$ $= [\text{SB}(\text{OH})_3]^- - \text{K}^+ + 2\text{H}_2\text{O}$	$K_1^* = \frac{([\text{SB}(\text{OH})_3]^- - \text{K}^+)^0}{[\text{SOH}][\text{B}(\text{OH})_3^0][\text{Ca}^{2+}]} \exp[F^*(\psi_\beta - \psi_0)]$
$2\text{SOH} + \text{B}(\text{OH})_4^- + \text{H}^+$ $= [(\text{SO})_2\text{B}(\text{OH})]^{0+} + 3\text{H}_2\text{O}$	$K_2^* = \frac{[(\text{SO})_2\text{B}(\text{OH})]^{0+}}{[\text{SOH}]^2[\text{B}(\text{OH})_4^-][\text{H}^+]}$
$\text{SOH} + \text{B}(\text{OH})_4^- + \text{K}^+$ $= [\text{SOB}(\text{OH})_3]^- - \text{K}^+ + \text{H}_2\text{O}$	$K_3^* = \frac{([\text{SOB}(\text{OH})_3]^- - \text{K}^+)}{[\text{SOH}][\text{B}(\text{OH})_4^-][\text{K}^+]} \exp[F^*(\psi_\beta - \psi_0)]$
$\text{SOH} + \text{B}(\text{OH})_3^0 + \text{Ca}^{2+}$ $= [\text{SB}(\text{OH})_3]^- - (\text{CaOH})^+ + 2\text{H}_2\text{O}$	$K_4^* = \frac{[\text{SB}(\text{OH})_3]^- - [\text{CaOH}]^+}{[\text{SOH}][\text{B}(\text{OH})_3^0][\text{Ca}^{2+}]} \exp[F^*(\psi_\beta - \psi_0)]$
$2\text{SOH} + \text{B}(\text{OH})_4^- + \text{CaOH}^+$ $= [\text{SO}_2\text{B}(\text{OH})_2]^- - (\text{CaOH})^+ + 2\text{H}_2\text{O}$	$K_5^* = \frac{[\text{SO}_2\text{B}(\text{OH})_2]^- - (\text{CaOH})^+}{[\text{SOH}]^2[\text{B}(\text{OH})_4^-][\text{CaOH}^+]} \exp[F^*(\psi_\beta - \psi_0)]$
$\text{XOH} + \text{B}(\text{OH})_4^- + \text{CaOH}^+$ $= [\text{XO}^- \text{Ca}^{2+}]^+ - \text{B}(\text{OH})_4^- + \text{H}_2\text{O}$	$K_6^* = \frac{[\text{XO}^- \text{Ca}^{2+}]^+ - \text{B}(\text{OH})_4^-^0}{[\text{XOH}][\text{B}(\text{OH})_4^-][\text{CaOH}^+]} \exp[F^*(\psi_0 - \psi_\beta)]$

S, X = aluminol, silanol sites.

$F^* = (F/RT)$ .

#### van Bemmelen-Freundlich isotherm

The composite Freundlich isotherm (Figure 5) also provides a good linear trend for both the electrolytes. Correlations for  $n$  greater and less than 0.5 were evaluated before selecting the value of  $n$  equal to 0.5. The constant,  $n$ , is related to the distribution of the bond strengths. If  $n = 1$ , all surface sites are equivalent and the isotherm reduces to the Langmuir form where  $\Gamma_{\text{max}} \rightarrow \infty$ . For  $n > 1$ , the surface bond energy distribution varies over a wide range. For  $n < 1$  in the case of  $n = 0.5$ , bond energies increase with the adsorption density. The edge positive sites are pH-dependent and limited. The boron concentrations are low and the divalent calcium either in the ion-pair or as an adsorbed species on the silanol site enhances the adsorption, or creates new sites for the negatively-charged borate ion.

#### Triple-layer surface-complexation model

The location of ions, either as inner-sphere (surface coordination or outer-sphere (ion-pair) complexes, results in intrinsic constants and activity coefficients based on different interactions with interfacial potential. Due to the consideration of specific adsorption of the electrolyte ions and multiple-layer structure, the TL(g)-SCM or TL-SCM in FITEQL (Westall, 1982) has two basic features that are not part of the simpler models derived from the basic Stern model. The intrinsic constants are applicable over a wide range of ionic strengths, and in this paper these constants are valid over a wide boron concentration range. Of all of the surface-complexation models, the TL-SCM has been used to describe electrokinetic potential of oxides quantitatively (Yates *et al.*, 1974; Davis *et al.*, 1978). Electrokinetic



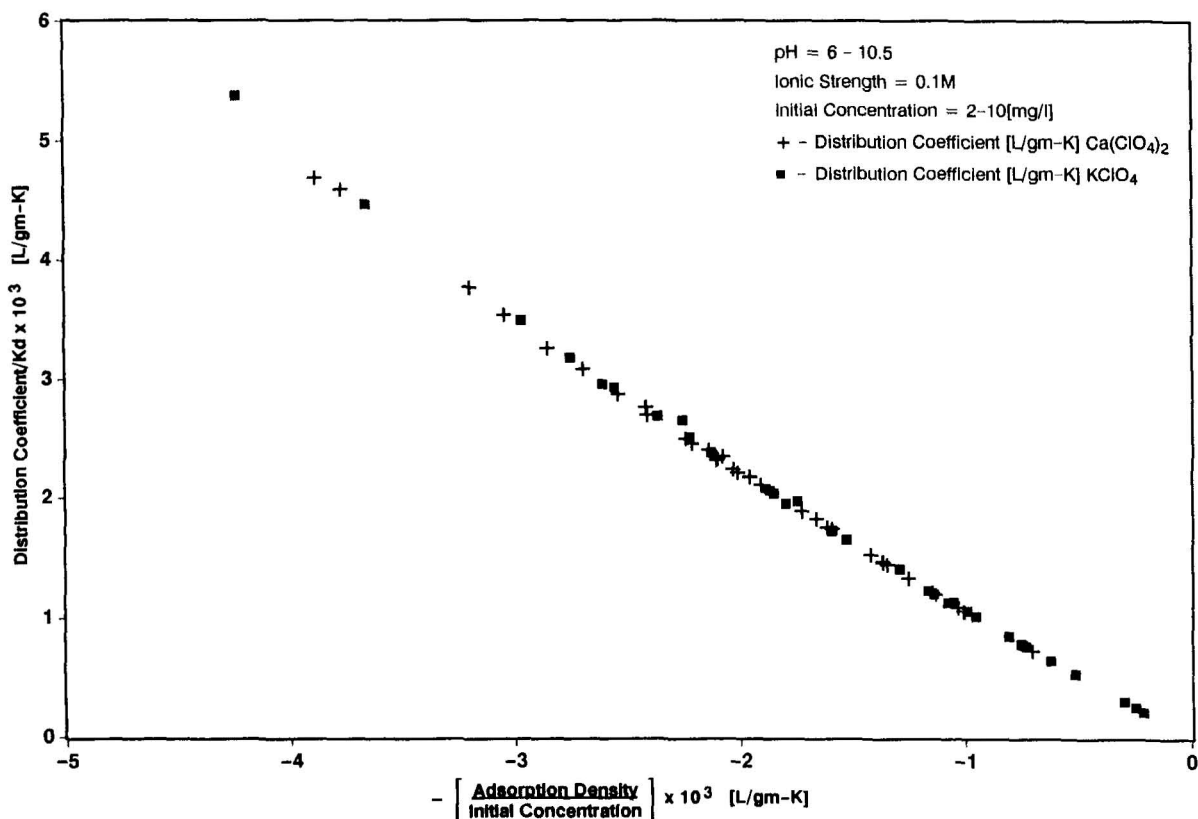


Figure 4. Langmuir isotherm for boron adsorption for  $\text{KClO}_4$  and  $\text{Ca}(\text{ClO}_4)_2$  electrolytes.

data for kaolinite in different background electrolyte and boron adsorption are nonexistent. At this stage, modeling of the electrokinetic phenomenon is probably feasible, but without the applicable data, it is impossible.

The experiments conducted by Mattigod *et al.* (1985) were not specifically designed for the application of the triple-layer model. These experiments were conducted to evaluate the effect of ion-pair formation on boron adsorption on kaolinite. Ideally, the coefficients of the

individual adsorbing species would be extracted from the experiment conducted on the substrate. The parameters required in the model were collected from the published literature, since specific data was not available from the experiments.

Equilibrium computation of boron speciation in equilibrated solutions indicates predominance of boric acid,  $\text{B}(\text{OH})_3^0$  in both of the electrolytes below pH 7. Above this pH, the effect of the ion-pair is explicitly apparent. In the 0.1 M  $\text{KClO}_4^0$  medium for all experiments, maximum concentration of  $\text{KB}(\text{OH})_4^0$  did not exceed 5% of the total boron concentration in the solution. The cation species  $\text{CaB}(\text{OH})_4^+$  in 0.033 M  $\text{Ca}(\text{ClO}_4)_2$  constituted approximately 45% of the solution.  $\text{B}(\text{OH})_4^-$  species concentration was reduced from 95% in  $\text{KClO}_4$  electrolyte to approximately 55% in the  $\text{Ca}(\text{ClO}_4)_2$  medium. Both inner- and outer-sphere complexes were used to study boron adsorption. The site descriptions were chosen either as single or bidentate complexations to fit the experimental data. One inner-sphere complex, and a hybrid of the outer and the inner sphere for comparison, were modeled in order to simulate the adsorption isotherms. Various reaction schemes were attempted, but are not presented since they do not provide any more understanding than those

Table 5. Linear regression coefficients for phenomenological models.

Parameters	Langmuir	van Bemmelen-Freundlich
X	$\Gamma/C_i$	$C_e/C_i$
Y	$K_d$	$K_d$
Slope	$k_L \cdot C_i$	$k_F \cdot C_i^{(1/n)-1}$
	-1.232	-0.0262
Intercept	$k_L \cdot S_T$	$C_F$
	-0.0002	0.0258
$r^2$	0.9956	0.9558

$C_e$  = equilibrium concentration,  $C_i$  = initial [total] concentration,  $\Gamma$  = adsorption density,  $K_d$  = distribution coefficient,  $k_L$  = Langmuir constant,  $k_F$  and  $1/n$  = van Bemmelen-Freundlich parameters.

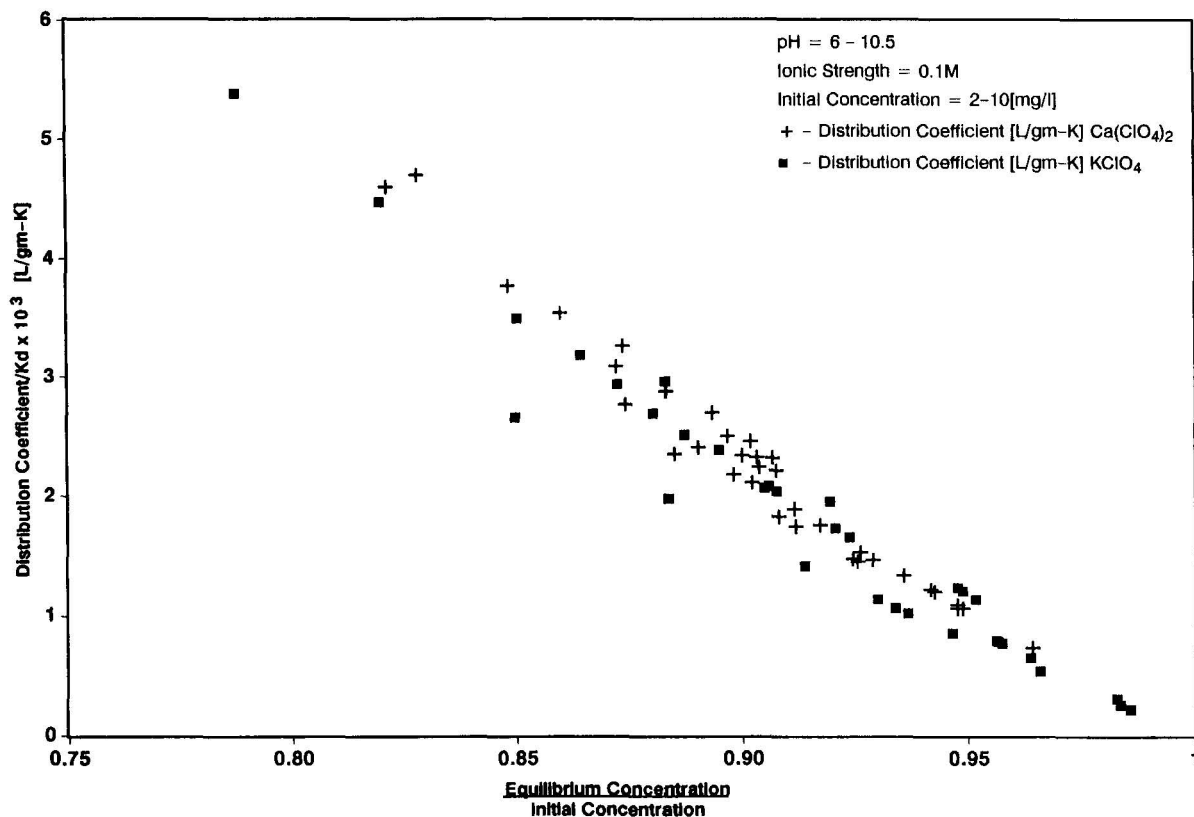


Figure 5. van Bemmelen-Freundlich isotherm for boron adsorption for  $\text{KClO}_4$  and  $\text{Ca}(\text{ClO}_4)_2$  electrolytes.

delineated in Table 4. The outer-sphere complexation reaction using  $\text{B}(\text{OH})_4^-$  provided a fair fit over the 7.5–9.5 pH range, but prediction outside this range was less than the experimental results.

Postulated surface reactions were based on possible chemical interaction at the surface. The adsorbing species on the aluminol and silanol sites are not close analogs of the solution species. The final choices of the surface-complexation reactions are identified in Table 4. The intrinsic equilibrium surface-complexation constants were computed independently for each set of the experimental data. A sensitivity study on capacitances and sites produced a variation of chemical equilibrium constants within a 5% range. The experimental data and the curves derived from the TL(g)-SCM are presented in Figures 6 and 7. The intrinsic equilibrium surface-complexation constants for the reactions, which were obtained by the application of the model using FITEQL, are tabulated in Table 6. The large deviation between the experimental data and the computed curves can be partially attributed to the combination of uncertainty of the published and experimental data used for the computation of the intrinsic equilibrium constant in the model. Boron adsorption envelopes for both the background electrolytes (Figures 8, 9) were

created using the equilibrium constants in Table 6. Isoadsorption curves (Figures 10, 11) were generated as contour plots from the boron adsorption envelopes (Figures 8, 9). These isoadsorption plots show contours of equal adsorption as a function of pH and initial B concentrations. Various combinations of pH and initial B concentrations that would produce the same amount of adsorption on the surface can be read from these plots.

#### Maximum boron adsorption

Maximum boron adsorption has been observed between pH 8.5 and 9.0, close to the  $\text{pK}_a$  of boric acid in an ionic strength solution of 0.1 M  $\text{KClO}_4$  or  $\text{Ca}(\text{ClO}_4)_2$  electrolyte (Mattigod *et al.*, 1985). Similar

Table 6. Intrinsic equilibrium constants.

Constants	log K
$K_1^*$	$3.57 \pm 0.48$
$K_2^*$	$14.81 \pm 0.19$
$K_3^*$	$19.32 \pm 0.13$
$K_4^*$	$0.37 \pm 0.39$
$K_5^*$	$-3.67 \pm 1.34$
$K_6^*$	$13.07 \pm 0.06$



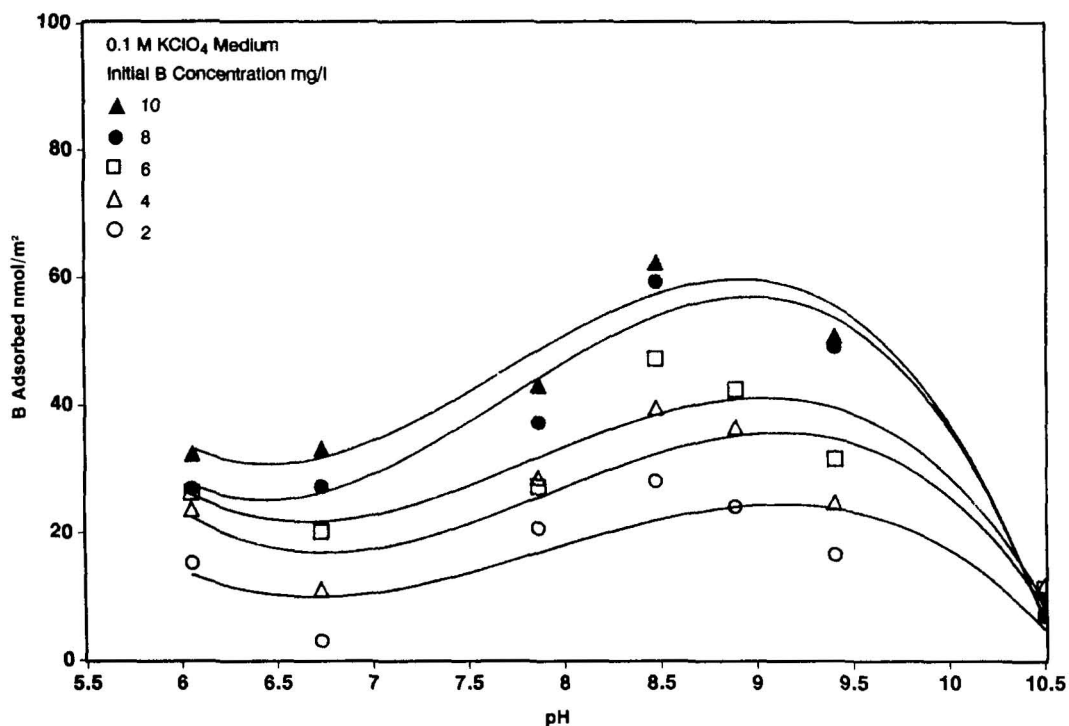


Figure 6. Adsorption density vs pH for the TL(g)-SCM and the experimental data for boron adsorption on kaolinite in  $\text{KClO}_4$  electrolyte.

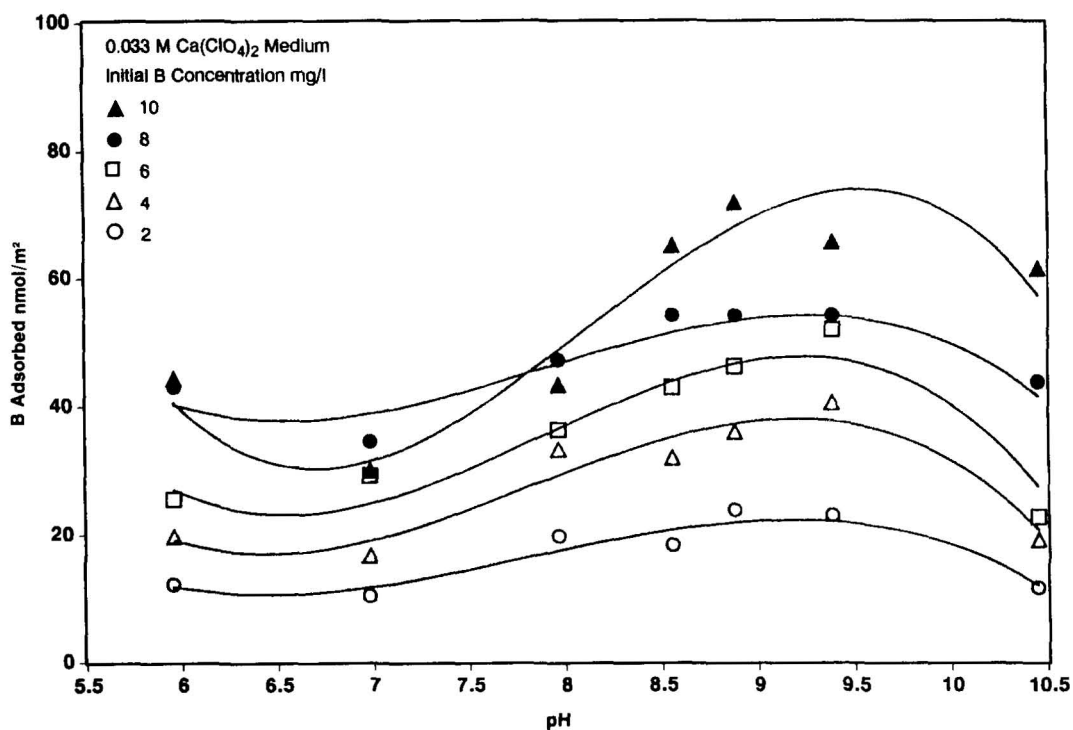


Figure 7. Adsorption density vs pH for the TL(g)-SCM and experimental data for boron adsorption on kaolinite in  $\text{Ca}(\text{ClO}_4)_2$  electrolyte.

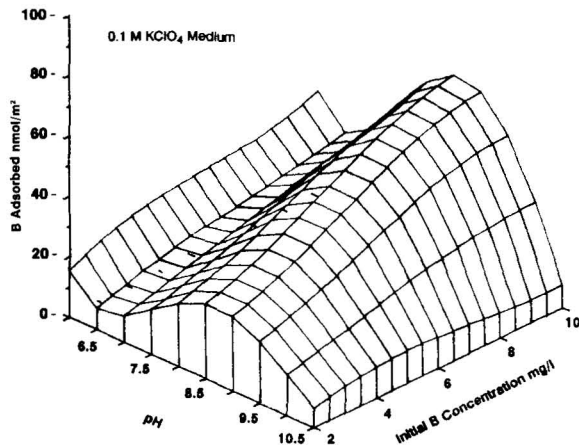


Figure 8. Boron adsorption envelope ( $\text{KClO}_4$  medium).

observations were reported by Hingston (1964), Sims and Bingham (1967), Keren and Mezuman (1981), and Goldberg and Glaubig (1986). The maximum adsorption occurs close to the  $\text{pK}_a$  (Hingston *et al.*, 1967), since boric acid is easily deprotonated within the EDL at the hydroxylated surface to replace the newly-formed surface water molecules. Based on the above reasoning, Hingston *et al.* (1967) hypothesized that the maximum adsorption of a weak acid is determined by the probability of the base and its conjugate occurring in equal proportions. The above mechanism of boron adsorption is widely accepted as specific adsorption by ligand exchange (Sposito, 1984) and interpreted by Keren and Mezuman (1981), in terms of affinity parameters, as competing effects of the boron species and the hydroxyl ions for surface sites. The difference between the experimental and the computed values of pH for maximum boron adsorption may be the result of the sparse experimental data and the inherent uncertainty in the published data used in the triple-layer model.

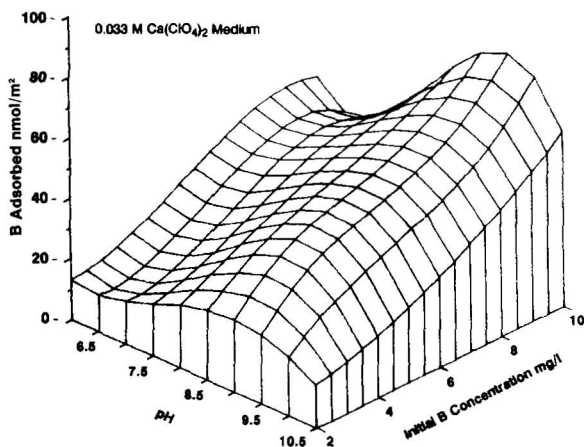


Figure 9. Boron adsorption envelope [ $\text{Ca}(\text{ClO}_4)_2$  medium].

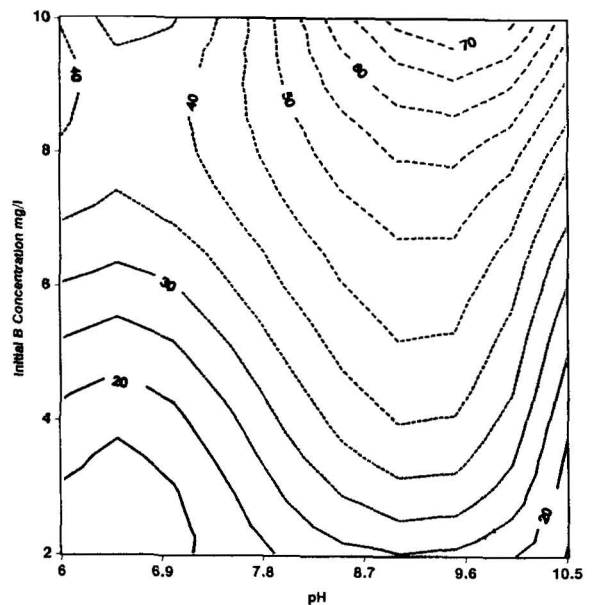


Figure 10. Boron isoadsorption ( $\text{nM}/\text{m}^2$ ) curves for boron ( $\text{KClO}_4$  medium).

## CONCLUSIONS

The phenomenological equations exhibited linear trends over a large portion of the data range. The weak nonlinear behavior occurred at high distribution coefficients or adsorption density, which could be attributed to the ion-pair and exchangeable cation effects. The equations have provided supporting evidence of

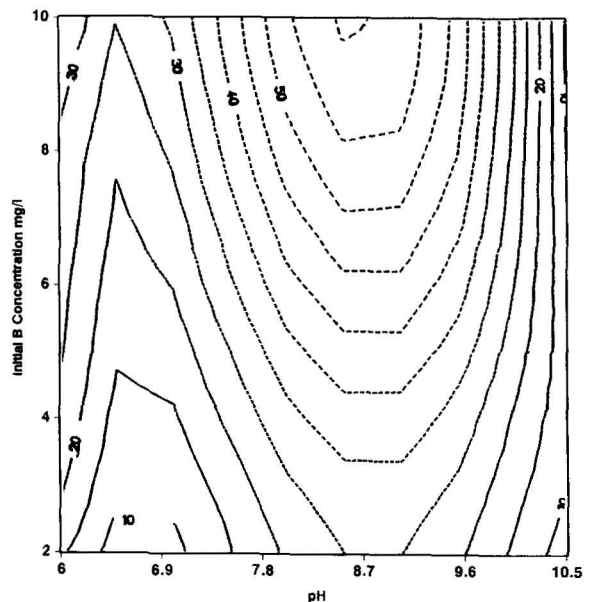


Figure 11. Boron isoadsorption ( $\text{nM}/\text{m}^2$ ) curves for boron [ $\text{Ca}(\text{ClO}_4)_2$  medium].



the phenomenon affecting increased boron adsorption in  $\text{Ca}(\text{ClO}_4)_2$  electrolyte. However, explicit formulations of the plausible surface reactions and computations of the intrinsic equilibrium constants were only feasible using the TL(g)-SCM. The TL(g)-SCM requires a large input of data, which must be directly applicable to the substrate in order to provide accurate modeling. The model is more complex than the phenomenological equations, but provides a better understanding of the plausible reactions of the solute within the solvent/substrate interface. Finally, an observation must be made regarding reporting of surface reactions and surface complex formation constants. Absolute values of surface reaction constants and the location of ions within the surface/solution interface must be regarded with caution. Such assertions are consistent with experimental data, but they are by no means the only possible interpretation unless substantiated by experimental observations. "Intrinsic" equilibrium constants have been found by extrapolation of data to zero charge, where the electrostatic energy term vanishes. The extrapolation of data for determining the "intrinsic" equilibrium constant is influenced by the assumptions of the physical and the electrostatic properties of the substrate/solution interface. Within the limitations of the concept of the original experiment and the use of the published data not specific to the substrate, the TL(g)-SCM does provide insight that can be further explored with specifically-designed experiments for application of the triple-layer model. To provide a meaningful comparison the models are provided along with the constants.

#### ACKNOWLEDGMENTS

Helpful discussions were provided by Drs. J. M. Zachara and C. E. Cowan (Battelle, Pacific Northwest Laboratories, Richland, Washington) and Dr. J. C. Westall (Oregon State University, Corvallis, Oregon). Constructive review was provided by Dr. L. Criscenti (Battelle, Pacific Northwest Laboratories). Significant help in manuscript preparation was provided by Kern and Kush Singh. Laurel Grove (Battelle, Pacific Northwest Laboratories) provided editorial assistance. Mr. J. A. Emmanuelli (United Engineers and Constructors, Englewood, Colorado) provided assistance with the text and graphics. The senior author completed this work during his tenure as a University of Washington NORCUS appointee at Battelle, Pacific Northwest Laboratories.

#### REFERENCES

- Alwitt, R. S. (1972) The point of zero charge of pseudo-boehmite: *J. Colloid Interface Sci.* **40**, 195–198.
- Baes, C. F., Jr. and Mesmer, R. E. (1976) *The Hydrolysis of Cations*: John Wiley, New York, 489 pp.
- Balistreri, L. and Murray, J. W. (1979) Surface of goethite in seawater: in *Chemical Modelling in Aqueous Systems*, E. A. Jenne, ed., *ACS Symposium Series* **93**, Washington, D.C., 275–298.
- Bassett, R. L. (1976) *The Geochemistry of Boron in Thermal Waters*: Doctoral thesis, Stanford University, Stanford, California, 290 pp.
- Beyrouthy, C. A., van Scoyoc, G. E., and Feldkamp, J. R. (1984) Evidence supporting specific adsorption of boron on synthetic aluminum hydroxides: *Soil Sci. Soc. Am. J.* **48**, 284–287.
- Blesa, M. A., Maroto, A. J. G., and Regazzoni, A. E. (1984) Boric acid adsorption on magnetite and zirconium dioxide: *J. Colloid Interface Sci.* **99**, 32–40.
- Byrne, R. H. and Kester, D. R. (1974) Inorganic speciation of boron in sea water: *J. Mar. Res.* **32**, 119–127.
- Chan, D., Perram, J. W., and White, L. R. (1975) Regulation of surface potential of amphoteric surfaces during particle-particle interaction: *J. Chem. Soc. Faraday Trans.* **171**, 1046–1057.
- Davies, C. W. (1962) *Ion Association*: Butterworths, London, 189 pp.
- Davis, J. A., James R. O., and Leckie, J. O. (1978) Surface ionization and complexation at the oxide/water interface. 1. Computation of electrical double layer properties in simple electrolytes: *J. Colloid Interface Sci.* **63**, 480–499.
- Davis, J. A. and Leckie, J. O. (1978) Surface ionization and complexation at the oxide/water interface. 2. Surface properties of amorphous iron oxyhydroxide and metal ions: *J. Colloid Interface Sci.* **67**, 90–107.
- Davis, J. A. and Leckie, J. O. (1979) Speciation of adsorbed ions at the oxide/water interface: in *Chemical Modelling in Aqueous Systems*, E. A. Jenne, ed., *ACS Symposium Series* **93**, Washington, D.C., 290–320.
- Davis, J. A. and Leckie, J. O. (1980) Surface ionization and complexation at the oxide/water interface. 3. Adsorption of anions: *J. Colloid Interface Sci.* **74**, 32–53.
- Fricke, R. and Leonhardt, I. (1950) Isoelectrischer Punkt und Pufferlösung: *Die Naturwissenschaften* **37**, 428.
- Goldberg, S. and Glaubig, R. A. (1985) Boron adsorption on aluminum and iron oxide minerals: *Soil Sci. Soc. Am. J.* **49**, 1374–1379.
- Goldberg, S. and Glaubig, R. A. (1986) Boron adsorption and silicon release by minerals kaolinite, montmorillonite, and illite: *Soil Sci. Soc. Am. J.* **50**, 1442–1448.
- Grahame, D. C. (1947) The electrical double layer and the theory of electrocapillarity: *Chem. Rev.* **41**, 441–501.
- Hachiya, K., Sasaki, M., Ikeda, T., Mikami, N., and Yasunaga, T. (1984) Static and kinetic studies of adsorption-desorption of metal ions on  $\gamma\text{-Al}_2\text{O}_3$  surface. 2. Kinetic study by means of pressure jump technique: *J. Phys. Chem.* **88**, 27–31.
- Hayes, K. F. and Leckie, J. O. (1986) Mechanism of lead, iron adsorption at the goethite water interface, Geochemical processes at mineral surfaces: *ACS Symposium Series* **323**, Chap. 7, 116–141.
- Hayes, K. F. and Leckie, J. O. (1987) Modelling ionic strength effects on cation adsorption at the hydrous oxide/solution interface: *J. Colloid Interface Sci.* **115**, 564–572.
- Hayes, K. F., Papelis, C., and Leckie, J. O. (1988) Modelling ionic strength effects on anion adsorption at hydrous oxide/solution interfaces: *J. Colloid Interface Sci.* **125**, 717–726.
- Hingston, F. J. (1964) Reactions between boron and clays: *Aust. J. Soil Res.* **2**, 83–95.
- Hingston, F. J., Atkinson, R. J., Posner, A. M., and Quirk, J. P. (1967) Specific adsorption of anions: *Nature* **215**, 1459–1461.
- Keren, R. and Mezuman, U. (1981) Boron adsorption by clay minerals using a phenomenological equation: *Clays & Clay Minerals* **29**, 198–204.
- Mattigod, S. V., Frampton, J. A., and Lim, C. H. (1985)

- Effect of ion-pair formation on boron adsorption by kaolinite: *Clays & Clay Minerals* **33**, 433–437.
- Mesmer, R. E., Baes, C. F., and Sweeton, F. H. (1972) Acidity measurements at elevated temperatures: *Inorg. Chem.* **11**, 537–543.
- Reardon, E. J. (1976) Dissociation constants for alkali earth and sodium borate ion pairs from 10° to 50°C: *Chem. Geol.* **18**, 309–325.
- Richter, R. (1987) *Chemical speciation of fly ash pond leachate in the underlying soil/water system with emphasis on the adsorption of nickel by oxides*: Doctoral thesis, Department of Civil Engineering, University of Notre Dame, South Bend, Indiana, 223 pp.
- Riese, A. C. (1982) *Adsorption of radium and thorium onto quartz and kaolinite, a comparison of solution/surface equilibria models*: Doctoral thesis, Colorado School of Mines, Golden, Colorado, 210 pp.
- Schindler, P. W. and H. Gamsjäger (1972) Acid-base reactions of TiO<sub>2</sub> suspensions: *Kolloid Z. Z. Polym.* **250**, 759–763.
- Sigg, L. and Stumm, W. (1981) The interaction of anions and weak acids with the hydrous goethite [ $\alpha$ -FeOOH] surface: *Colloid Surf.* **2**, 101–117.
- Sims, J. R. and Bingham, F. T. (1967) Retention of boron by layer silicates, sesquioxides, and soil minerals: I. Layer silicates: *Soil Sci. Soc. Amer. Proc.* **31**, 728–732.
- Sposito, G. (1984) *The Surface Chemistry of Soils*: Oxford Univ. Press, New York, 234 pp.
- Sposito, G., Holtzclaw, K. M., Johnston, C. T., and LeVeque-Madore, C. S. (1981) Thermodynamics of sodium-copper exchange on Wyoming bentonite at 298°K: *Soil Sci. Soc. Amer. J.* **47**, 51–56.
- Stumm, W., Hohl, H., and Dalang, F. (1976) Interaction of metal ions with hydrous oxide surfaces: *Croat. Chem. Acta.* **48**, 491–504.
- Stumm, W., Huang, C. P., and Jenkins, S. R. (1970) Specific chemical interaction affecting the stability of dispersed systems: *Croat. Chem. Acta.* **42**, 223–245.
- Stumm, W., Krummert, R., and Sigg, L. (1980) A ligand exchange model for the adsorption of inorganic and organic ligands at hydrous oxide interfaces: *Croat. Chem. Acta.* **53**, 291–312.
- Swallow, K. C., Hume, D. N., and Morel, F. M. M. (1980) Sorption of copper and lead by hydrous ferric oxide: *Environ. Sci. & Techn.* **14**, 1326–1331.
- Westall, J. C. (1982) *FITEQL: a computer program for determination of chemical equilibrium constants from experimental data*: **Rep. 82-01**, Dept. of Chemistry, Oregon State University, Corvallis.
- Yates, D. E., Levine, S. E., and Healy, T. W. (1974) Site-binding model of the electric double layer at the oxide/water interface: *J. Chem. Soc. Faraday Trans.* **70**, 1807–1818.
- Zachara, J. M., Cowan, C. E., Schmidt, R. L., and Ainsworth, C. C. (1988) Chromate adsorption by kaolinite: *Clays & Clay Minerals* **36**, 317–326.
- Zachara, J. M., Girvin, D. C., Schmidt, R. I., and Resch, C. T. (1987) Chromate adsorption on amorphous iron oxyhydroxide in presence of major groundwater ions: *Environ. Sci. & Techn.* **21**, 589–594.

(Received 14 June 1991; accepted 17 December 1991; Ms. 2113)